Magnetism of an ultrathin Mn film on Co(100) and the effect of oxidation studied by x-ray magnetic circular dichroism

Yoshiki Yonamoto, Toshihiko Yokoyama,* Kenta Amemiya, Daiju Matsumura,
and Toshiaki Ohta

Department of Chemistry, Graduate School of Science, The University of Tokyo, 7-3-1 Hongo, Bunkyo-ku, Tokyo 113-0033, Japan

The electronic and magnetic structures of a Mn ultrathin film grown on a 3-ML (monolayer) Co film have been investigated during stepwise oxidation by means of O K-, Mn $L_{III,II}$-, and Co $L_{III,II}$-edge x-ray-absorption spectroscopy and Mn $L_{III,II}$-, and Co $L_{III,II}$-edge x-ray magnetic circular dichroism (XMCD). Without O_2, strong interaction between the Mn and Co $3d$ orbitals was suggested and Mn-Co ferromagnetic coupling was confirmed. We observed significant suppression of the d hole number and the spin and orbital moments of Co after Mn deposition compared to those before Mn deposition. These findings imply that the Mn d electrons are transferred to the minority-spin levels of Co. At 0.5-L (Langmuir) O_2 exposure, the spin and orbital moments of Co do not change noticeably, while the Mn $L_{III,II}$-edge XMCD almost completely vanishes. After 5.5-L O_2 exposure, an antiparallel spin alignment between Mn and Co was observed. The estimated orbital moments of Mn is reduced from 0.06 (before oxidation) to $<0.005\mu_B$ (after oxidation). It is concluded that unoxidized Mn is in the $d^5 + d^6$ state while oxidized Mn is in the d^5 high-spin state. Such variance of the electron configuration of Mn can explain the unusual magnetic properties. Antiferromagnetic coupling between Co and oxidized Mn may originate from the d^5 high-spin configuration of Mn rather than from the superexchange interaction between Mn and Co via the O atom.

I. INTRODUCTION

Thin $3d$ transition-metal films often show enhanced magnetic moments compared to those in bulk materials.[1,2] Among them, ultrathin Mn films have been of interest because Mn forms an ideally two-dimensional surface alloy and the magnetic property is considered to affect geometric structure strongly. During the last decade, many experimental and theoretical studies have been performed in order to clarify the relation between the magnetism and structure of the Mn films such as Mn/Cu(100),[3–11] Mn/Cu(110),[12,13] Mn/Cu(111),[14] Mn/Ni(100),[10–12,15,16] Mn/bcc-Fe(100),[2,12,17–30] Mn/fcc-Co(100),[6,31–35] and Mn/Pt (111).[36] These investigations suggest that the 0.5-ML (monolayer) Mn film deposited at room temperature forms a $c(2\times2)$ substitutional alloy,[3–5,10,11,16,21,34,35] where half of the outermost layer of the substrate is substituted by Mn.

Although the formation of the surface alloy has been observed for many other systems such as Au/Cu(100) and Pd/Cu(100), the Mn surface alloy exhibits considerably large buckling. LEED (low-energy electron diffraction) experiments indicated that the amounts of the buckling are 0.30 and 0.25 Å for Mn/Cu and Mn/Ni, while they are 0.10 and 0.02 Å for Au/Cu and Pd/Cu, respectively.[7] Such a large difference cannot be explained only by the variance of the atomic radii, so that the magnetic property of Mn should be taken into account.

A theoretical study concerning the relation between structure and magnetism revealed that the driving force for the large surface buckling is the enhancement of the Mn magnetic moment.[7] Recently, O'Brien and Tonner comparatively investigated the Mn films grown on Cu(100) and Ni(100).[10] They observed a large buckling on both the substrates, while the ferromagnetic alignment in the Mn film was found only on Ni, indicating that the large structural change cannot be attributed to the ferromagnetic alignment. They also found an enhancement of the Mn magnetic moment caused by the localization of the Mn $3d$ orbital for both Mn/Cu and Mn/Ni. It was concluded that Mn is in the high-spin (HS) d^5 state and that the buckling originates from the increasing atomic radii of Mn due to the change in electronic structure.

An attractive subject was whether the magnetic moment of the Mn film is parallel or antiparallel with respect to that of the substrate and what kind of mechanism works on the magnetic coupling. Many investigations using XMCD[12,17,20,22] (x-ray magnetic circular dichroism), spin-resolved x-ray photoelectron spectroscopy,[25] spin-polarized electron energy-loss spectroscopy,[24] and theoretical calculations[18,21,30] for Mn/Fe films showed an antiferromagnetic coupling, whereas Andrieu *et al.* found ferromagnetic interaction.[26] O'Brien, Zhang, and Tonner also suggested that the Mn/Co film shows ferromagnetic coupling.[6,31] On the other hand, Noguera *et al.* obtained no ferromagnetic solutions in their calculations using a tight-binding Hamiltonian.[32]

These discrepancies between experiments can now be explained by the effect of oxidation. Recent XMCD studies on both the Mn/Fe (Ref. 29) and Mn/Co (Ref. 33) films indicated that observed antiferromagnetic coupling between Mn and Fe (or Co) is just due to oxidation of the Mn films. Although ferromagnetic coupling was observed just after the deposition, the magnetic coupling was found to be reversed as oxidation of the Mn film proceeded. They concluded that antiferromagnetic Mn-Co interaction originates from MnO, while ferromagnetic Mn-Co interaction is attributed to bare Mn. It is interesting that in the Mn/Co and Mn/Fe films the Mn-Mn interaction is ferromagnetic not only for MnO but

also for bare Mn, because the bulk MnO and Mn metal are both antiferromagnets. Andrieu *et al.*[29] suggested that antiferromagnetic Mn-Co coupling originates from superexchange interaction via oxygen atoms, although the mechanism of the magnetic coupling has not yet been understood because of the lack of detailed electronic and structural information. It can be expected that the change in the Mn electronic configuration due to oxygen exposure causes the magnetic coupling reversal. The magnetic and electronic properties of the Mn film and the effect of oxidation deserves much more attention.

Stimulated by these investigations, we have in the present work studied O_2+Mn/Co/Cu(100) by means of O K-, Mn $L_{III,II}$-, and Co $L_{III,II}$-edge x-ray-absorption spectroscopy (XAS) and XMCD techniques. The aims of the present study are as follows. First, we will confirm the reversal of the magnetization of Mn films by oxidation by measuring the Mn $L_{III,II}$-edge XAS and XMCD spectra before and after oxygen exposure. This is a reexamination of the previous studies.[29,33] Second, we will investigate the change of electronic and magnetic properties of Co between before and after Mn deposition by recording the Co $L_{III,II}$-edge XAS and XMCD spectra as well. In the previous studies,[29,33] the Co films employed might be too thick to detect any change. We chose Co thickness of 3 ML, which is thin enough to observe the electronic change of the Co films. Third, by measuring the O K-edge XAS, we will identify the oxide species formed that could be dependent on the O coverage. Consequently, from the observed XAS and XMCD spectra for the Mn films, we will clarify the close correlation between magnetism and electronic structure and will conclude that the variance of the $3d$-electron number of Mn causes these unusual magnetic properties.

II. EXPERIMENTS

A Mn ultrathin film was prepared on a Co thin film grown on a Cu(100) single crystal according to the following procedure. The Cu(100) substrate was cleaned by repeated cycles of Ar^+ ion bombardment and annealed at 920 K in an ultrahigh vacuum chamber. Sample annealing was performed by electron bombardment from the rear side of the crystal and the temperature was monitored with a chromel-alumel thermocouple. No contamination was observed by XAS and the order of the surface was confirmed by reflection high-energy electron diffraction (RHEED). A 3-ML Co film was grown at 300 K on Cu(100) by evaporation from a resistively heated Co wire. The morphology and growth mode were monitored by *in situ* RHEED observation. Distinct oscillations were observed up to 3 ML, confirming the layer-by-layer growth of a fcc Co film. An ultrathin Mn film was subsequently grown at the substrate temperature of 300 K by resistively heating a W cage containing small Mn fractions. The Mn coverage was chosen to be (0.4 ± 0.1) ML.

The structure of the film and the deposition rate of Mn had been checked in another ultrahigh vacuum chamber equipped with LEED optics prior to the spectroscopic experiment. After the Mn evaporation, a $c(2\times 2)$ LEED pattern with a little higher background was observed, this being

consistent with the previous report.[34] A little higher background is possibly attributed to the formation of small Mn islands. We estimated the deposition rate of Mn by assuming that the 0.5-ML Mn film gives the sharpest $c(2\times 2)$ LEED pattern. Only a (1×1) LEED pattern originating from the substrate could be observed after oxygen exposure.

All the spectroscopic measurements were performed at the beamline 11A of the Photon Factory in the Institute of Materials Structure Science, High Energy Accelerator Research Organization (KEK-PF).[37–40] We employed x rays with a positive helicity by setting the slit 0.4 ± 0.1 mrad above the synchrotron orbit plane. The circular polarization factor was estimated to be $P_c=0.60$ by measuring the total electron yield Co $L_{III,II}$-edge XMCD spectra of bulk Co prepared *in situ*. All the spectra of the thin Mn/Co films were recorded in a partial electron yield mode using a detector consisting of a 25-mm diameter microchannel plate (MCP) and two Au-coated W grids that were placed just below the sample. Retarding voltages (-400, -450, and -500 V for O K, Mn L, and Co L edges, respectively) were applied to the second grid (closer to the MCP), while the first one was grounded.

The XMCD spectra were obtained by reversing the magnetization of the film leaving the helicity of the incident x rays unchanged. Since the Co films investigated here are known to be magnetized along the surface plane,[33] the grazing-incidence ($\theta=30°$ or $150°$) XMCD spectra were recorded. Here θ is the angle between the magnetization and the x-ray wave vector. In this paper, XMCD is defined as the difference between two spectra with the photon helicity parallel (σ_+) and antiparallel (σ_-) to the majority spin of the sample, while XAS is given by ($\sigma_+ + \sigma_-$)/2. The saturation effect originating from the self-absorption of x rays[41] is negligible for the thin film investigated here.

III. RESULTS AND DISCUSSION

A. Co $L_{III,II}$-edge XMCD

Figure 1 shows the Co $L_{III,II}$ edge circularly polarized and XMCD spectra of a 3-ML Co film, taken before and after the deposition of 0.4-ML Mn. Although the features of the circularly polarized spectra were almost unchanged by Mn deposition, a considerable decrease in the peak intensities was observed especially at the L_{III} edge; when the average is taken between the σ_+ and σ_- spectra in Fig. 1, the maximum absorption at the L_{III} edge is ~4.09 before Mn deposition and reduced to ~3.92 after Mn deposition. Since the peak intensity is proportional to the $3d$ hole number, this implies a decrease in the Co $3d$ hole that can be attributed to electron transfer from Mn toward Co. Moreover, the L_{III} peak of the spin antiparallel spectrum (σ_-) shows a larger decrease (the maximum absorption is reduced from ~4.49–~4.21), while the σ_+ spectrum changed slightly (the maximum absorption is reduced from ~3.69–~3.63), suggesting that only the Co $3d$ minority-spin ($\downarrow$) hole decreases by Mn deposition. This can be interpreted to mean that the ($\downarrow$) electrons of Mn are transferred to the Co ($\downarrow$) hole. Since the magnetic moment of Co originates from the unpaired $3d$ ($\uparrow$)
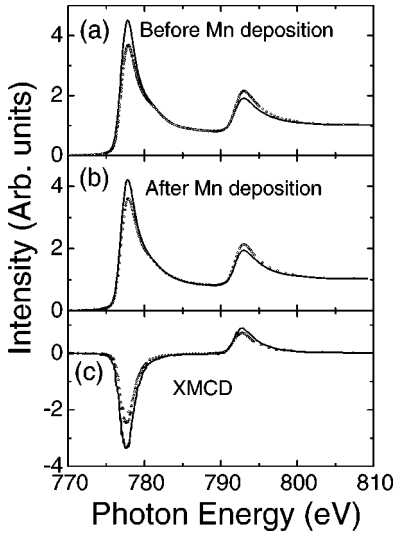
FIG. 1. (a) and (b) Co $L_{\mathrm{III,II}}$-edge circularly polarized spectra of 3-ML Co film before and after Mn deposition. Solid lines and open circles, respectively, correspond to the spin antiparallel (σ_-) and parallel (σ_+) spectra (a) before and (b) after Mn deposition. (c) Co $L_{\mathrm{III,II}}$-edge XMCD spectra taken before (solid line) and after (open triangles) Mn deposition.

FIG. 2. Mn $L_{\mathrm{III,II}}$-edge XAS spectra taken with increasing oxygen exposure, together with the Mn^{2+} high-spin (HS) atomic calculation. The bulk Mn spectrum is also shown for comparison.

electrons and is limited by the number of $3d$ holes, this charge transfer causes a large decrease in the Co $L_{\mathrm{III,II}}$-edge XMCD intensity.

For quantitative discussion, the number of d holes n_d must be known. This can be estimated from the integrated intensity of the XAS white line. Since the saturation effect (self-absorption effect) of bulk Co cannot be neglected, the spectra were modified by assuming infinite thickness of bulk Co and the electron escape depth of 25 Å.[41] By using n_d = 2.50 for bulk Co,[42] we obtained n_d = 2.39 and 2.21 for Co films before and after Mn deposition, respectively. This decrease clearly supports the charge transfer described above. The results of the numerical analyses using the well-established sum rules[43–45] are summarized in Fig. 5 (shown later), which confirm the decrease in both the spin and orbital magnetic moments of Co due to Mn deposition.

Similar spin moment changes caused by charge transfer have also been reported for other thin metal films. Recent studies on Ni/Co systems, where the electron transfers from Co to Ni, have revealed the enhancement of the spin moments for Co.[46,47] On the contrary, theoretical studies for Mn/Co and Mn/Fe have shown suppression of the moments of the substrates,[2,32,48] in accordance with our finding. As for the orbital moment, the situation is different. The orbital moment is usually strongly dependent on environment, so that simple discussion cannot be applied. It is safe to remark, however, that Mn is a strong magnetic killer for the substrate.[2,32,48]

Next, the Mn/Co film was dosed with 0.5- and subsequently 5.0-L O$_2$. We found slight changes in the Co $L_{\mathrm{III,II}}$-edge XMCD spectra, consistent with the previous work.[33] Both the spin and orbital moments are almost unchanged after 0.5-L O$_2$ exposure, but slightly decrease after 5.5-L O$_2$, as shown later in Fig. 5. Taking into consideration
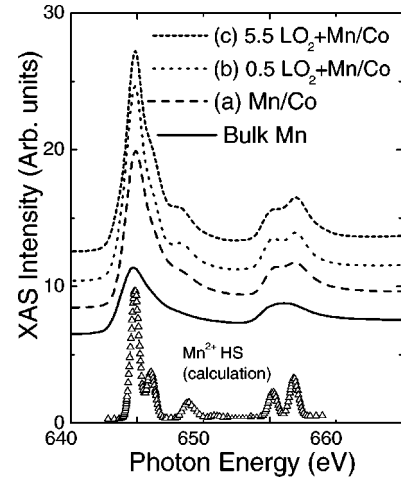
the fact that bulk cobalt oxide is an antiferromagnetic material, the Mn film should preferably be oxidized prior to the Co substrate, and excess oxygen subsequently reacts with Co around 5.5-L exposure.

B. Mn $L_{\mathrm{III,II}}$-edge and O K-edge XAS

Figure 2 shows the Mn $L_{\mathrm{III,II}}$-edge XAS spectra taken with increasing O$_2$ exposure (0, 0.5, and 5.5 L), together with that of bulk Mn. The XAS peak intensity for bare Mn [Fig. 1(a)] is much larger than that of bulk, which implies a significant difference in the electronic configuration between the film and bulk Mn. In order to investigate the electronic structure of the Mn film, we estimate the branching ratio for the Mn $L_{\mathrm{III,II}}$-edge XAS spectra.[5,12,49,50] Here the branching ratio is defined by $R_B = (\int L_{\mathrm{III}})/(\int L_{\mathrm{II}} + \int L_{\mathrm{III}})$, where $\int L_{\mathrm{II}}$ and $\int L_{\mathrm{III}}$ are the integrated intensities of the L_{II} and L_{III} white lines, respectively, obtained after subtracting the background. We estimated the error for R_B to be less than 0.05.

As indicated in Fig. 2, the estimated R_B for the Mn film is 0.79 before O$_2$ exposure [Fig. 2(a)], which is consistent with the previous study for Mn/Cu(100).[12] R_B for a nearly half filled $3d$ shell such as Mn is strongly influenced by electrostatic interaction and is very sensitive to the change in electronic structure. In fact, it reaches the maximum value of ~0.8 for the d^5 high-spin (HS) state,[49] while it is 0.73 for bulk Mn ($d^5 + d^6 + d^7$).[51] Accordingly, the R_B value obtained here (0.79) suggests that the electronic configuration of the bare Mn film is close to the d^5 HS state. This can be explained by the strength of interaction between Mn atoms. For bulk, the electronic configuration is $d^5 + d^6 + d^7$ and the R_B is smaller due to strong Mn-Mn interaction.[51] In the case of the present film, the Mn-Mn interaction is considerably weaker and the Mn $3d$ orbital is more localized because of the $c(2 \times 2)$ structure,[4] leading to a nearly d^5 HS state.[29,33,50,52,53] This interpretation is supported by the fact that vapor Mn with no interaction shows characteristics of a pure d^5 HS state.[52] The observed XAS line shape is, however, broader than that of vapor Mn.[52] This can be attributed
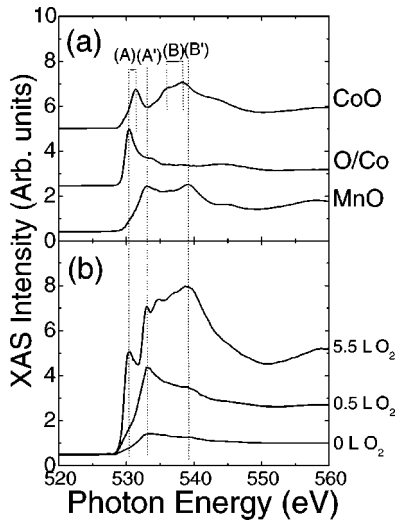
FIG. 3. (a) O K-edge XAS spectra of CoO, oxygen adsorbed on Co (O/Co) and MnO. (b) O K-edge XAS spectra of Mn/Co (0-L O_2), 0.5-L O_2+Mn/Co, and 5.5-L O_2+Mn/Co.

to strong Mn-Co interaction that makes Mn $3d$ states itinerant, indicating that the electron number is slightly larger than five.

After exposure to 0.5-L O_2, the Mn $L_{\mathrm{III,II}}$-edge XAS spectrum [Fig. 2(b)] shows some multiplet peaks, narrowing of peaks, and a small increase in R_B (to 0.8). This implies that the Mn $3d$ orbital is more localized and closer to a pure d^5 HS state compared to the bare Mn film. Moreover, the Mn $L_{\mathrm{III,II}}$-edge XAS for 5.5-L O_2 [Fig. 2(c)] shows excellent agreement with the calculated spectrum for atomic Mn^{2+} with the d^5 HS state,[51–54] implying that there is little Mn-Co hybridization and MnO is dominant.

In order to obtain information on the oxidation state, we measured the O K-edge XAS spectra. They are shown in Fig. 3, together with those for bulk MnO and CoO films, and oxygen adsorbed on Co(100) (O/Co) for comparison.[55] It is known that the XAS spectra of $3d$ transition-metal oxides exhibit double peaks labeled (A') and (B') for MnO in Fig. 3.[56–58] The former (A) or (A') is attributed to the transition to the hybridized orbital between O $2p$ and metal $3d$, while the latter (B) or (B') originates from O $2p$ and metal $4sp$. Peak (B) was not observed for O/Co because the spectrum was measured with grazing x-ray incidence and the transition moment for peak (B) is nearly parallel to the surface plane.[59]

As can be seen in Fig. 3, a small O-K XAS signal was observed even at 0-L oxygen (as deposited). This may be mainly due to residual CO in the UHV chamber as previously pointed out.[29,33] The presence of peaks (A') and (B') means that a small part of Mn is already oxidized to MnO. Note that other Mn oxides such as Mn_2O_3 and MnO_2 show no peaks around these energies.[56–58] After the 0.5-L oxygen exposure, peaks (A') and (B') can clearly be observed, while peak (A) does not appear. This also implies that only MnO is present and the Co film is not yet oxidized. Peak (A) appears only after 5.5-L O_2 exposure, the energy of which is identical to that of O/Co. The oxidation state of Mn is con-
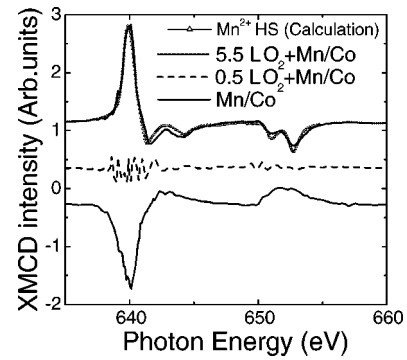

FIG. 4. Mn $L_{\mathrm{III,II}}$-edge XMCD spectra taken with increasing oxygen exposure, together with the Mn^{2+} HS atomic calculation.

sidered to be divalent because of the presence of peaks (A') and (B'), consistent with the results of the Mn $L_{\mathrm{III,II}}$-edge XAS spectra.

C. Induced moment on Mn

The Mn $L_{\mathrm{III,II}}$-edge XMCD spectra are shown in Fig. 4, where one can clearly find significant changes caused by oxygen exposure. For 0-L O_2, the XMCD shows a negative sign at the L_{III} edge. Although a theoretical study for Mn/Co indicates that the magnetic moment of Mn is antiparallel to that of substrate Co,[32] the observed XMCD spectrum clearly implies ferromagnetic coupling between the Mn and Co films. After 0.5-L O_2 exposure, the XMCD almost completely vanished. Moreover, a clear XMCD signal with an opposite sign reappeared by subsequent exposure to further 5.0-L O_2 (5.5 L in total). These observations are all consistent with the previous experimental works on the Mn/Co system by O'Brien, Zhang, and Tonner,[6,31,33] and are also in good accordance with the ones on the Mn/Fe system.[29] In Fig. 4, the Mn $L_{\mathrm{III,II}}$-edge XMCD spectrum from the Mn^{2+} d^5 HS atomic calculations[50,52–54] is also depicted, which agrees well with that for 5.5-L O_2. This confirms that MnO is formed at 5.5-L O_2 exposure. It is concluded that the Mn/Co film (corresponding to 0-L O_2) shows ferromagnetic Mn-Co coupling, while the MnO/Co case (5.5-L O_2) shows antiferromagnetic Mn-Co interaction. As for 0.5-L O_2, where the XMCD signal vanishes, it is appropriate to recognize that half of the Mn film is oxidized and the XMCD signal of the MnO film is canceled with that of unoxidized Mn. In fact, similar disappearance of the XMCD signal was reported for Mn/Fe and the ratio of oxygen with respect to Mn was found to be 0.5 when the XMCD signal vanishes.[29]

Although the reason for the reversal of the magnetic coupling has been an open question, Andrieu *et al.* attributed it to the superexchange Mn-Co interaction via oxygen atoms.[29] Both MnO and CoO are typical antiferromagnetic materials with rocksalt structure. They show a parallel spin alignment within the (111) plane, while the magnetic moment of each layer aligns antiferromagnetically. Accordingly, the coupling between Mn and Co should be antiparallel if the Mn-O-Co bond were formed and the surface should show a (111) facet. In such a situation, however, a considerable change in the Co $L_{\mathrm{III,II}}$-edge XMCD spectra should be observed because of the

Co-O bond formation as well as the Mn-O one. This contradicts our present observation as described above. We can thus propose here that the reversal of the magnetic coupling is caused by the change in Mn electronic structure (the $d^5 + d^6$ state to a d^5 HS state) rather than by the superexchange Mn-O-Co interaction. A detailed discussion will be given below after obtaining the spin and orbital moments of Co and Mn. It should also be noted here that the appearance of Mn $L_{III,II}$-edge XMCD signals means that the Mn-Mn coupling in both the Mn and MnO films is ferromagnetic, whereas it is antiferromagnetic in the bulk. For bulk Mn, the antiferromagnetism originates from strong interaction between Mn atoms.[21,30] On the contrary, the Mn and MnO films have only weak Mn-Mn interaction because of a longer Mn-Mn distance and a smaller coordination number. Therefore, Mn-Co interaction could induce ferromagnetic coupling between Mn atoms for both the bare and oxidized Mn films.

In order to clarify the mechanism of the magnetic-moment reversal, we performed a numerical analysis for the spin and orbital moments on Mn. Unfortunately, the usual spin sum rule[44,45] cannot be applied directly to the Mn $L_{III,II}$-edge XMCD spectra because of overlap of the $2p_{3/2}$ and $2p_{1/2}$ levels (jj coupling). Although the previous study[33] ignored the coupling, this should be important because the spin sum rule is rigorously correct in the case of no jj coupling. It was suggested that the sum rule considerably underestimates the spin magnetic moment on Mn due to significant jj coupling.[60] The spin moment obtained by using the usual sum rule should thus be multiplied by a compensation factor χ. Previous studies[12,60] indicate $\chi \sim 1.5$.

Another problem is that the sum rule analysis requires a standard sample with known moments. Bulk Mn is, however, an antiferromagnetic material and there is no adequate standard for Mn. Therefore, we utilize the transferability rule proposed by Samant et al.[61] The spin moment derived from the sum rule[44] can be expressed as

$$C|M_{pd}|^2 m_s = \int L_{III} - 2 \int L_{II}, \qquad (1)$$

where C is the constant depending on the angular moments of the p and d shells. M_{pd} and m_s are the radial transition matrix element and the spin magnetic moment, respectively. The equation can be rewritten by using compensation factor χ:

$$m_s = \frac{\chi}{C^*}\left(\int L_{II} - 2\int L_{II}\right), \qquad (2)$$

where $C^* = C|M_{pd}|^2$ and $\chi \sim 1.5$.[12,60] According to the transferability rule,[61] M_{pd} is transferable for atoms with similar atomic numbers and one can assume that C^* for Mn is almost identical to that for Co. Since C^* can be easily estimated from a bulk Co spectrum, one can determine the Mn spin magnetic moment. The orbital magnetic moment can be described as well:

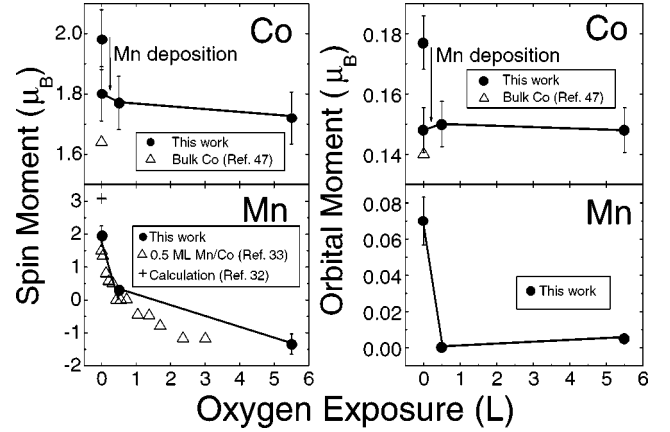$$m_l = \frac{1}{B^*}\left(\int L_{III} + \int L_{II}\right). \qquad (3)$$

FIG. 5. Results of the numerical analyses of magnetic moments (in units of μ_B) for Co and Mn films, together with reference values. Experimental and analytical errors were estimated and the resultant total error bars containing inaccuracy of the transferability rule are given.

Again assuming that B^* is the same for Mn and Co, one can obtain both m_s and m_l. In the present case, bare Mn is dominantly in the d^5 HS state and MnO is purely in the d^5 HS state. This indicates that the transferability rule can be similarly applied to both phases with similar accuracy.

The obtained values for m_s and m_l are indicated in Fig. 5. The sign of m_s for the MnO film (5.5-L O_2) is opposite to that for the Mn film (0-L O_2), as mentioned above. As for the size of the magnetic moment, Noguera et al.[32] predicted theoretically that m_s for the Mn film is $\sim 3\mu_B$, which is significantly larger than our result. One possible reason for this difference can be found in the structure of the Mn film. They calculated with the assumption that Mn does not form an alloy with Co but grows as a complete monolayer film, while our LEED pattern supports the alloy formation. We cannot rule out, however, the possibility of an island formation. Because bulk Mn is an antiferromagnet, the island formation[3] should reduce the spin moment m_s observed as an average over the whole Mn film. Another possible reason is the oxidation as mentioned above. Since the magnetic moment of MnO is opposite to that of Mn, even a small amount of oxidation greatly affects the observed m_s value. Moreover, it must be taken into account that the XMCD spectra were measured at 300 K, which might be too high for the film to be magnetically saturated.

As for the orbital moments, it should be emphasized that m_l for the Mn film (0-L O_2) is $0.06\mu_B$, while it is quite small ($\sim 0.005\mu_B$) for the MnO film (5.5 L). Note that these values are possibly underestimated as mentioned above. According to the Hund rule, the orbital angular momentum should be parallel to the spin angular momentum if the $3d$ subshell is occupied by more than five electrons, while m_l should be zero in a pure d^5 state. Therefore, the positive m_l value for the Mn film implies that the electron configuration is not pure d^5 but is mixed with d^6. In contrast, the MnO film seems to be almost in a pure d^5 state. The spectral shapes of XAS also suggest the difference in electronic structure between the Mn and MnO films; rather broad peaks

were observed for Mn due to hybridization with Co, whereas the XAS for MnO showed sharper peaks because of the decrease in hybridization.

Many previous studies showed that Mn couples ferromagnetically with Fe or Co hosts, while Cr shows antiferromagnetic coupling.[2,62–64] This is explained as follows. In early transition metals such as Mn, the $3d$ states are located at higher energies than those of Fe or Co because the nuclear charge pulls $3d$ electrons stronger in later transition metals. The minority-spin ($\downarrow$) levels in Fe or Co are more unstable than the majority one ($\uparrow$) due to the exchange splitting. Therefore, the ($\downarrow$) electrons in Fe or Co can be hybridized more significantly with the electrons of early transition-metal atoms, leading to antiferromagnetic coupling. If the guest is a late transition metal, the situation is reversed and ferromagnetic coupling is preferred. The reversal of magnetic coupling occurs between Mn ($n_d \sim 6$) and Cr ($n_d \sim 5$).[48] In the present case, the electron configuration of the bare Mn film corresponds to $n_d > 5$, leading to ferromagnetic coupling. On the contrary, the Mn atom of the MnO film is in the pure d^5 state ($n_d = 5$) and could show antiferromagnetic coupling as do early transition metals with $n_d < 5$. Consequently, we can remark that the reversal of the Mn magnetic moment upon oxygen exposure should be derived from the change in the electronic configurations from the $d^5 + d^6$ state to d^5, rather than Mn-Co superexchange interaction via oxygen.

IV. CONCLUSIONS

We have studied the magnetic behavior of a Mn ultrathin film grown on a Co(100) surface with increasing oxygen exposure by using XAS and XMCD. It was found that the magnetic moment on Co is significantly reduced by Mn deposition. This is attributed to hybridization between Co and Mn $3d$ orbitals. The Mn d electrons are transferred to the minority-spin levels of Co. The Mn film showed ferromagnetic coupling with the substrate and a considerable change was observed in the electronic configuration compared to bulk Mn. Oxygen preferably reacts with Mn and the MnO film is formed, which is also ferromagnetic with other Mn atoms but is antiferromagnetic to the Co substrate. Ferromagnetic Mn-Mn coupling in the Mn and MnO films implies that Mn-Mn interaction is weaker compared to a bulk Mn metal and that Mn-Co interaction is predominant.

We performed numerical analyses for the Mn $L_{III,II}$-edge XMCD spectra by using the sum rule and the transferability rule. It was indicated that the electron configuration of the bare Mn film is the d^5 HS state with a little mixing of d^6, while the MnO film shows a pure d^5 HS state. This change in the electronic configuration should cause the reversal of the Mn magnetic moment upon oxygen exposure, rather than superexchange interaction between Mn and Co via oxygen. The present study has revealed interesting magnetic properties of the Mn film in the oxidation process and suggested a close relation between magnetism and electronic configuration. Proper quantitative structural investigations and more refined theoretical calculations including oxygen are needed for a more detailed discussion.

*Electronic address: toshi@chem.s.u-tokyo.ac.jp

[1] S. Blügel, B. Drittler, R. Zeller, and P. H. Dederichs, Appl. Phys. A: Solids Surf. **49**, 547 (1989).

[2] S. Mirbt, O. Eriksson, and B. Johansson, Phys. Rev. B **52**, 15 070 (1995).

[3] D. Jeon, H. P. Noh, T. Hashizume, Y. Kuk, and T. Sakurai, Appl. Surf. Sci. **87/88**, 386 (1995).

[4] T. Flores, M. Hansen, and M. Wuttig, Surf. Sci. **279**, 251 (1992).

[5] F. Schiller, Y. Huttel, J. Avila, and M. C. Asensio, Surf. Sci. **433-435**, 434 (1999).

[6] W. L. O'Brien, J. Zhang, and B. P. Tonner, J. Phys.: Condens. Matter **5**, L515 (1993).

[7] S. Blügel, Appl. Phys. A: Mater. Sci. Process. **63**, 595 (1996).

[8] M. Eder, J. Hafner, and E. G. Moroni, Surf. Sci. **423**, L244 (1999).

[9] M. Eder, J. Hafner, and E. G. Moroni, Phys. Rev. B **61**, 11 492 (2000).

[10] W. L. O'Brien and B. P. Tonner, Phys. Rev. B **51**, 617 (1995).

[11] O. Rader, W. Gudat, C. Carbone, E. Vescovo, S. Blügel, R. Kläsges, W. Eberhardt, M. Wuttig, J. Redinger, and F. J. Himpsel, Phys. Rev. B **55**, 5404 (1997).

[12] H. A. Dürr, G. van der Laan, D. Spanke, F. U. Hillebrecht, N. B. Brookes, and J. B. Goedkoop, Phys. Rev. B **56**, 8156 (1997).

[13] H. A. Dürr, G. van der Laan, D. Spanke, F. U. Hillebrecht, N. B. Brookes, and J. B. Goedkoop, Surf. Sci. **377-379**, 466 (1997).

[14] D. Spišák and J. Hafner, Phys. Rev. B **61**, 12 728 (2000).

[15] D. Schmitz, O. Rader, C. Carbone, and W. Eberhardt, Phys. Rev. B **54**, 15 352 (1996).

[16] M. Wuttig, T. Flores, and C. C. Knight, Phys. Rev. B **48**, 12 082 (1993).

[17] O. Rader, W. Gudat, D. Schmitz, C. Carbone, and W. Eberhardt, Phys. Rev. B **56**, 5053 (1997).

[18] M. Taguchi, O. Elmouhssine, C. Demangeat, and J. C. Parlebas, Phys. Rev. B **60**, 6273 (1999).

[19] T. Igel, R. Pfandzelter, and H. Winter, Phys. Rev. B **58**, 2430 (1998).

[20] J. Dresselhaus, D. Spanke, F. U. Hillebrecht, E. Kisker, G. van der Laan, J. B. Goedkoop, and N. B. Brooks, Phys. Rev. B **56**, 5461 (1997).

[21] Ruqian Wu and A. J. Freeman, Phys. Rev. B **51**, 17 131 (1995).

[22] J. Dresselhaus, D. Spanke, F. U. Hillebrecht, E. Kisker, G. van der Laan, J. B. Goedkoop, and N. B. Brooks, Surf. Sci. **377-379**, 450 (1997).

[23] R. Pfandzetler, T. Igel, and H. Winter, Surf. Sci. **389**, 317 (1997).

[24] T. G. Walker and H. Hopster, Phys. Rev. B **48**, 3563 (1993).

[25] Ch. Roth, Th. Kleeman, F. U. Hillebrecht, and E. Kisher, Phys. Rev. B **52**, R15 691 (1995).

[26] S. Andrieu, M. Finazzi, Ph. Bauer, H. Fischer, P. Lefevre, A. Traverse, K. Hricovini, G. Krill, and M. Piecuch, Phys. Rev. B **57**, 1985 (1998).

[27] S. Bouarab, H. Nit-Laziz, M. A. Khan, C. Demangeat, H. Dreysse, and M. Benakki, Phys. Rev. B **52**, 10 127 (1995).

[28] D. Spišák and J. Hafner, Phys. Rev. B **55**, 8304 (1997).

[29] S. Andrieu, E. Foy, H. Fischer, M. Alnot, F. Chevrier, G. Krill, and M. Piecuch, Phys. Rev. B **58**, 8210 (1998).

[30] Ruqian Wu and A. J. Freeman, J. Magn. Magn. Mater. **161**, 89 (1996).

[31] W. L. O'Brien and B. P. Tonner, Phys. Rev. B **50**, 2963 (1994).

[32] A. Noguera, S. Bouarab, A. Mokrani, C. Demangeat, and H. Dreyssé, J. Magn. Magn. Mater. **156**, 21 (1996).

[33] W. L. O'Brien and B. P. Tonner, Phys. Rev. B **58**, 3191 (1998).

[34] B.-Ch. Choi, P. J. Bode, and J. A. C. Bland, Phys. Rev. B **59**, 7029 (1999).

[35] B.-Ch. Choi, P. J. Bode, and J. A. C. Bland, J. Appl. Phys. **85**, 5063 (1999).

[36] S. Gallego, L. Chico, and M. C. Muñoz, Phys. Rev. B **57**, 4863 (1998).

[37] K. Amemiya, Y. Kitajima, T. Ohta, and K. Ito, J. Synchrotron Radiat. **3**, 282 (1996).

[38] K. Amemiya, Y. Kitajima, Y. Yonamoto, T. Ohta, K. Ito, K. Sano, T. Nagano, M. Koeda, H. Sasai, and Y. Harada, Proc. SPIE **3150**, 171 (1997).

[39] Y. Kitajima, K. Amemiya, Y. Yonamoto, T. Ohta, T. Kikuchi, T. Kosuge, A. Toyoshima, and K. Ito, J. Synchrotron Radiat. **5**, 729 (1998).

[40] Y. Kitajima, Y. Yonamoto, K. Amemiya, H. Tsukabayashi, T. Ohta, and K. Ito, J. Electron Spectrosc. Relat. Phenom. **101-103**, 927 (1999).

[41] R. Nakajima, J. Stöhr, and Y. U. Idzerda, Phys. Rev. B **59**, 6421 (1999).

[42] O. Eriksson, B. Johansson, R. C. Albers, A. M. Boring, and M. S. S. Brooks, Phys. Rev. B **42**, 2707 (1990).

[43] B. T. Thole, P. Carra, F. Sette, and G. van der Laan, Phys. Rev. Lett. **68**, 1943 (1992).

[44] P. Carra, B. T. Thole, M. Altarelli, and X. Wang, Phys. Rev. Lett. **70**, 694 (1993).

[45] C. T. Chen, Y. U. Idzerda, H. J. Lin, N. V. Smith, G. Meigs, E. Chaban, G. H. Ho, E. Pellegrin, and F. Sette, Phys. Rev. Lett. **75**, 152 (1995).

[46] S. S. Dhesi, H. A. Dürr, E. Dudzik, G. van der Laan, and N. B. Brookes, Phys. Rev. B **61**, 6866 (2000).

[47] S. S. Dhesi, H. A. Dürr, G. van der Laan, E. Dudzik, and N. B. Brookes, Phys. Rev. B **60**, 12 852 (1999).

[48] H. Itoh, J. Inoue, and S. Maesaka, Phys. Rev. B **47**, 5809 (1993).

[49] B. T. Thole and G. van der Laan, Phys. Rev. B **38**, 3158 (1988).

[50] G. van der Laan and B. T. Thole, Phys. Rev. B **43**, 13 401 (1991).

[51] R. D. Cowan, *The Theory of Atomic Structure and Spectra* (University of California, Berkeley, 1981).

[52] U. Arp, F. Federmann, E. Källne, B. Sonntag, and S. L. Sorensen, J. Phys. B **25**, 3747 (1992).

[53] B. T. Thole, R. D. Cowan, G. A. Sawatzky, J. Fink, and J. C. Fuggle, Phys. Rev. B **31**, 6856 (1985).

[54] A. Kimura, S. Suga, T. Shishidou, S. Imada, T. Muro, S. Y. Park, T. Miyahara, T. Kaneko, and T. Kanomata, Phys. Rev. B **56**, 6021 (1997).

[55] K. Amemiya, T. Yokoyama, Y. Yonamoto, D. Matsumura, and T. Ohta (unpublished).

[56] H. Kurata and C. Colliex, Phys. Rev. B **48**, 2102 (1993).

[57] F. M. F. de Groot, M. Grioni, J. C. Fuggle, J. Ghijsen, G. A. Sawatzky, and H. Petersen, Phys. Rev. B **40**, 5715 (1989).

[58] H. Kurata, E. Lefèvre, C. Colliex, and R. Brydson, Phys. Rev. B **47**, 13 763 (1993).

[59] F. May, M. Tischer, D. Arvanitis, M. Russo, J. Hunter Dunn, H. Henneken, H. Wende, R. Chauvistré, N. Mårtensson, and K. Baberschke, Phys. Rev. B **53**, 1076 (1996).

[60] Y. Tanemura, A. Tanaka, and T. Jo, J. Phys. Soc. Jpn. **65**, 1053 (1996).

[61] M. G. Samant, J. Stöhr, S. S. P. Parkin, G. A. Held, B. D. Hermsmeier, F. Herman, M. van Schilfgaarde, L.-C. Duda, D. C. Mancini, N. Wassdahl, and R. Nakajima, Phys. Rev. Lett. **72**, 1112 (1994).

[62] S. Blügel, H. Akai, R. Zeller, and P. H. Dederichs, Phys. Rev. B **35**, 3271 (1987).

[63] B. Dritter, N. Stefanou, S. Blügel, R. Zeller, and P. H. Dederichs, Phys. Rev. B **40**, 8203 (1989), and references therein.

[64] T. Böske, W. Clements, C. Carbone, and W. Eberhardt, Phys. Rev. B **49**, 4003 (1994).